

Proton switch for modulating oxygen reduction by a copper electrocatalyst embedded in a hybrid bilayer membrane

Christopher J. Barile^{1†}, Edmund C. M. Tse^{1†}, Ying Li¹, Thomas B. Sobyra¹, Steven C. Zimmerman¹, Ali Hosseini² and Andrew A. Gewirth^{1,3*}

Molecular switches gate many fundamental processes in natural and artificial systems. Here, we report the development of an electrochemical platform in which a proton carrier switches the activity of a catalyst. By incorporating an alkyl phosphate in the lipid layer of a hybrid bilayer membrane, we regulate proton transport to a Cu-based molecular oxygen reduction reaction catalyst. To construct this hybrid bilayer membrane system, we prepare an example of a synthetic Cu oxygen reduction reaction catalyst that forms a self-assembled monolayer on Au surfaces. We then embed this Cu catalyst inside a hybrid bilayer membrane by depositing a monolayer of lipid on the self-assembled monolayer. We envisage that this electrochemical system can give a unique mechanistic insight not only into the oxygen reduction reaction, but into proton-coupled electron transfer in general.

Molecular switches regulate many functions in biology, chemistry and physics, and the development of artificial switches is an important goal in these fields. In nanotechnology, chemical switches are used in the construction of molecular machines^{1,2} and computers^{3,4}. In biological systems, switches are fundamental to gene regulation⁵, vision⁶ and cellular trafficking⁷. Frequently, such biological switches modulate proton transfer occurring in enzymes and across cellular membranes⁸. The protons regulated by these switches are frequently involved in proton-coupled electron transfer (PCET) reactions.

PCET reactions are also fundamental to many energy conversion processes such as N₂ fixation, H₂O oxidation and CO₂ reduction^{9–12}. The four-electron four-proton oxygen reduction reaction (ORR) to water is one of the most intensely studied reactions involving PCET (ref. 13). Much experimental and computational work examines the mechanism of the ORR in an effort to construct more efficient fuel cell cathodes¹³. However, in many cases, the mechanism of the ORR remains poorly understood.

At present, as proton transfer is hard to switch on and off, the effect of proton transfer on catalysis and other reactions cannot be easily evaluated. Traditionally, the pH of the bulk solution is varied to affect the thermodynamics of redox couples in the catalyst^{11,14–16}. The accompanying redox shift, however, gives little information about the influence of proton flux on the mechanism of the catalytic process. The role of covalently bound proton relays in ORR catalysts has also been explored^{17–19}. A hybrid bilayer membrane (HBM) is a unique electrochemical platform that can be used to interrogate the role of proton flux on a molecular ORR catalyst without altering either its molecular structure or the contents of the bulk solution²⁰. In a HBM system, a monolayer of lipid molecules is appended to a self-assembled monolayer (SAM) of alkanethiols covalently attached to a Au electrode^{21–24}. The role of proton flux in affecting the reactivity of a molecular ORR catalyst remains largely unexplored.

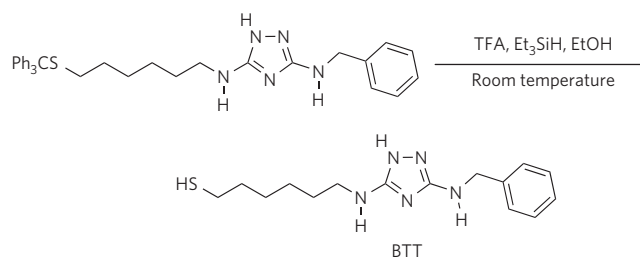


Figure 1 | Synthesis of BTT.

In this paper, we design and prepare a robust, active, dinuclear Cu ORR catalyst specifically tailored to be embedded inside a HBM system. We demonstrate that proton delivery to the catalyst through the lipid layer can be controlled through the use of an alkyl phosphate proton carrier and explore how this proton carrier can be used as a pH-sensitive switch.

Ligand design and synthesis

We designed a new ligand to support an active Cu O₂ reduction catalyst in a HBM system. Figure 1 and Supplementary Fig. 1 illustrate the preparation of 6-((3-(benzylamino)-1,2,4-triazol-5-yl)amino)hexane-1-thiol (BTT). The BTT ligand features three active regions, each with a specific function. The Cu coordination site is based on 3,5-diamino-1,2,4-triazole (DAT), which on coordination to Cu forms an efficient O₂ reduction catalyst over a wide pH range²⁵.

The second feature of BTT is a terminal benzyl moiety. Our initial attempts to deposit a lipid layer on a hydrophilic amino-terminated ligand were unsuccessful. We hypothesized that unfavourable interactions between the hydrophilic ends of the amino-terminated ligand and the hydrophobic tails of the lipid hinder the formation

¹Department of Chemistry, University of Illinois at Urbana-Champaign, Urbana, Illinois 61801, USA, ²Department of Chemical and Materials Engineering, The University of Auckland, Auckland 1010, New Zealand, ³International Institute for Carbon Neutral Energy Research (WPI-I2CNER), Kyushu University, Fukuoka 812-8581, Japan. †These authors contributed equally to this work. *e-mail: agewirth@illinois.edu

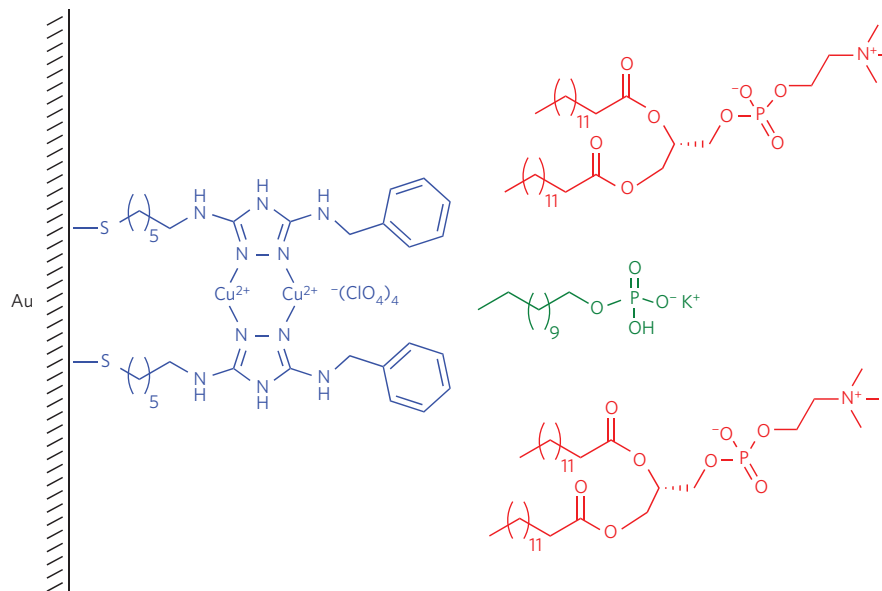


Figure 2 | Schematic of the hybrid bilayer membrane. The HBM used in this study is composed of the Cu complex of BTT (blue), the 1,2-dimyristoyl-*sn*-glycero-3-phosphocholine (DMPC) lipid layer (red), and the alkyl phosphate proton carrier (green).

of a HBM in this case. Therefore, we attached a hydrophobic benzyl moiety onto BTT to append the lipid layer, allowing us to construct the electrochemical platform described in Fig. 2.

Finally, we equipped BTT with a hexylthiol chain to allow the formation of a well-packed SAM on Au electrodes. Electron transfer through this short-chained thiol is facile, eliminating it as the rate-limiting step for O_2 reduction²⁶. A full monolayer of BTT on Au electrodes was formed through the *in situ* deprotection of the tritylated thiol using trifluoroacetic acid and triethylsilane (Fig. 1; ref. 27). O_2 reduction on the BTT-Au surface is greatly suppressed compared to a bare Au surface, demonstrating that the SAM layer is well formed and effectively passivates the Au electrode (Supplementary Fig. 2).

Oxygen reduction catalysis

To form an active O_2 reduction catalyst, we subsequently immersed the BTT-Au surface in a solution of $Cu(ClO_4)_2$ to form a dinuclear Cu complex with two triazole units. Scanning tunneling microscopy (STM) reveals that the roughness of the bare Au and BTT-Au surfaces with and without Cu do not deviate significantly, suggesting that the BTT monolayer is well packed and its uniformity is not perturbed by the addition of Cu (Supplementary Fig. 3). Ellipsometric measurements are also consistent with the formation of a full monolayer, as the length of the Cu complex of BTT on Au is 21 Å, comparable to the value obtained from theoretical modelling of the SAM (Supplementary Fig. 4).

O_2 reduction by the Cu complex of BTT on Au shows an onset potential of -70 mV versus Ag/AgCl at pH 7 (Fig. 3, blue curve). The Cu complex of BTT on Au reduces O_2 by an average of 3.7 ± 0.2 electrons, whereas a bare Au surface reduces O_2 by an average of 2.9 ± 0.1 electrons (Supplementary Fig. 5). The number of electrons by which O_2 is reduced and the onset potential of the Cu complex of BTT are similar to the values reported for the Cu complex of DAT on carbon black²⁵. These observations demonstrate that modifying the Cu complex of DAT with alkylthiol and benzyl moieties does not perturb its catalytic activity.

Under an argon atmosphere, the BTT-Au surface in the absence of Cu is redox-active (Supplementary Fig. 6, black curve). We hypothesize that this is due to the reversible one-electron reduction of the triazole ring, which has been reported for other triazole derivatives²⁸. Protected BTT (Supplementary Fig. 1, compound 4)

and DAT both exhibit redox waves at similar potentials in an ethanolic solution, further supporting this hypothesis (Supplementary Fig. 7). On the formation of the Cu complex on the BTT-Au surface, the charge under the redox wave nearly doubles (Supplementary Fig. 6, blue curve). This reflects an additional one-electron Cu(I)/Cu(II) couple occurring at a similar potential to the free BTT-Au wave. By correcting for the contribution of the BTT, the surface coverage of the Cu complex of BTT on Au is 3.4×10^{-11} mol cm^{-2} , which is similar to the value expected for a full monolayer (Supplementary Note 5). We note that the O_2 reduction onset potential of Cu BTT on Au is about 300 mV more negative than the Cu(I)/Cu(II) couple. This is expected as O_2 reduction is an inhibited process involving multiple proton delivery, electron transfer, and binding steps.

Hybrid bilayer membrane construction

To construct a platform containing a molecular switch, we embedded the catalyst in a lipid layer composed of 1,2-dimyristoyl-*sn*-glycero-3-phosphocholine (DMPC), which is stable in the pH 5–7 range, to form a HBM. Ellipsometric measurements demonstrate that the length of the appended lipid layer is 21 Å (Supplementary Fig. 4), and the double-layer current of the electrode decreases on formation of the HBM. These two findings are consistent with the formation of a well-formed DMPC monolayer (Supplementary Fig. 8; ref. 29). Supplementary Fig. 8 also shows that the amount of charge under the BTT and Cu(I)/Cu(II) waves decreases substantially on HBM formation. This behaviour arises because the anions ($H_2PO_4^-/HPO_4^{2-}$) from the aqueous–lipid interface are slow to diffuse through the lipid layer and compensate for the positive charge on the Cu complex, consistent with previous studies examining the transport properties of anions in HBM systems^{29,30}.

At pH 7, the addition of a lipid layer to the Cu complex shifts the onset potential for O_2 reduction ~ 300 mV negative relative to the onset of the Cu complex without lipid, significantly decreasing the catalytic current (Fig. 3, red curve). We hypothesize that the observed negative shift in the O_2 reduction onset potential is due to a change in the local environment of the catalyst from an aqueous medium to the hydrophobic lipid interior. O_2 reduction in the HBM is not limited by the diffusion of O_2 in DMPC because the diffusion coefficients of O_2 in DMPC and pH 7 buffer are comparable at

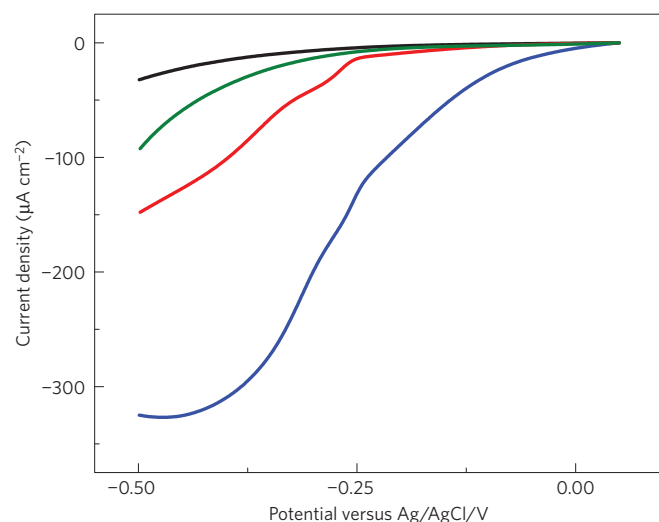


Figure 3 | pH 7 voltammetry. Linear sweep voltammograms of O_2 reduction by a SAM of the Cu complex of BTT (blue), the HBM containing the Cu complex with DMPC only in the lipid layer (red), the HBM containing the Cu complex with one equivalent of MDP incorporated in the lipid layer (green), and a BTT SAM (black) on Au at 26 °C in pH 7 buffer solution at a scan rate of 10 mV s⁻¹.

room temperature^{31–33}. Therefore, O_2 is expected to readily permeate through the lipid layer (Supplementary Note 6).

There are two remaining possibilities as to the origin of the decreased O_2 reduction rate in the HBM. These relate to inefficient delivery of either protons or electrons to the catalyst. The Cu complex of BTT without a lipid layer exhibits facile O_2 reduction, suggesting that electron delivery from the Au electrode is not rate determining in the HBM. Unlike O_2 , however, protons do not readily diffuse through the lipid layer of the HBM. In biological systems, protons are only shuttled across lipid bilayers with the aid of specific channels or mediators³⁴. This suggests that sluggish proton transfer through the lipid layer is responsible for the large negative shift of the onset potential for O_2 reduction by the catalyst when it is placed inside a HBM. Indeed, the slow and steady current rise we observe resembles the O_2 reduction profiles of Fe porphyrins appended to SAMs exhibiting slow electron transfer^{35,36}.

Proton carrier incorporation

We next incorporate an alkyl phosphate, mono-*N*-dodecyl phosphate (MDP), in our HBM system to facilitate proton transport to the embedded catalyst and to act as a molecular switch. Proton carriers, such as aliphatic acids and amines, orient themselves with their polar head groups towards the lipid–water interface³⁷. However, in the presence of a driving force such as a pH gradient, they deliver protons across the membrane via ‘flip–flop’ diffusion^{38,39}. Proton shuttling is important in many biological systems, such as mitochondrial membranes⁸. We incorporate MDP in the HBM as a unique proton carrier because it is diprotic and hence its ability to transport protons can be modulated by changes in pH, unlike previously used acids and amines. We confirm the presence of MDP in the lipid layer of the HBM using mass spectrometry (Supplementary Fig. 9). Figure 3 demonstrates that incorporating one equivalent of MDP into the lipid layer of the HBM inhibits the O_2 reduction activity of the Cu complex of BTT further at pH 7 (see green curve). At pH 7, MDP exists as an equilibrium mixture of $RHPO_4^-/RPO_4^{2-}$ (ref. 40). Protonation of this equilibrium mixture is dominated by the conversion of RPO_4^{2-} to $RHPO_4^-$. $RHPO_4^-$ is a poor proton carrier, as the transport of charged species through the hydrophobic interior of the lipid layer

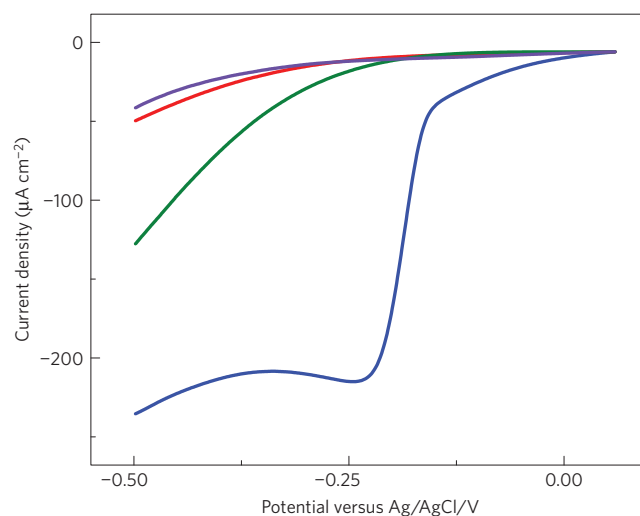


Figure 4 | pH 5 voltammetry. Linear sweep voltammograms of O_2 reduction by a SAM of the Cu complex at 26 °C (blue), the HBM containing the Cu complex with DMPC only in the lipid layer at 26 °C (red), and the HBM containing the Cu complex with one equivalent of MDP incorporated in the lipid layer at 26 °C (green) and 10 °C (purple) on Au in pH 5 buffer solution at a scan rate of 10 mV s⁻¹.

is energetically unfavourable³⁴. However, at pH 5, MDP exists predominantly as $RHPO_4^-$. This species can then be protonated to give neutral RH_2PO_4 , which can facilitate proton transport across the lipid layer of the HBM. This is confirmed by an increased O_2 reduction current by the embedded catalyst at pH 5 when one equivalent of MDP is incorporated in the lipid layer of the HBM (Fig. 4, green curve).

We hypothesize that the presence of MDP in the lipid layer increases the rate of proton delivery to the catalyst. Although the O_2 reduction current increases, it is not revived to the amount observed for the Cu complex of BTT without lipid because O_2 reduction inside the HBM is still limited by proton transport. However, the onset potential of the catalyst remains unchanged, suggesting that the incorporation of a proton carrier does not change the thermodynamics of the catalyst in the HBM system, but rather enhances the kinetics of proton transport.

To further interrogate the mechanism of proton transport inside the HBM, we studied the O_2 reduction activity of Cu BTT at 10 °C. At this temperature, DMPC monolayers exist in the gel phase⁴¹ where flip–flop diffusion is suppressed⁴², but the O_2 diffusion rate across the lipid layer is similar to that at room temperature (Supplementary Note 6). Unlike at 26 °C, the O_2 reduction current of the HBM with one equivalent of MDP at 10 °C (Fig. 4, purple curve) is similar to that of the HBM with DMPC only at 10 °C and 26 °C (Supplementary Fig. 10, red curve and Fig. 4, red curve). We hypothesize that because MDP cannot undergo flip–flop diffusion at 10 °C, it is not an effective proton carrier and hence does not enhance the O_2 reduction activity of the catalyst. However, when the surface is warmed to 26 °C after being cooled, MDP is reactivated as a proton carrier, resulting in revived O_2 reduction activity (Supplementary Fig. 10, green curve).

The integrity of the lipid layer is examined by blocking experiments with a solution of $K_3Fe(CN)_6$ (Supplementary Fig. 11; ref. 43). In the absence of the lipid layer, we observe a combination of Fe(II)/Fe(III), Cu(I)/Cu(II), and BTT redox couples in the cyclic voltammogram. The current significantly decreases on addition of DMPC, suggesting the presence of a well-packed monolayer of lipid on the SAM (ref. 43). More importantly, the current originating from the Fe(II)/Fe(III) couple is similar for both the lipid-only HBM and the HBM with MDP, indicating that the incorporation

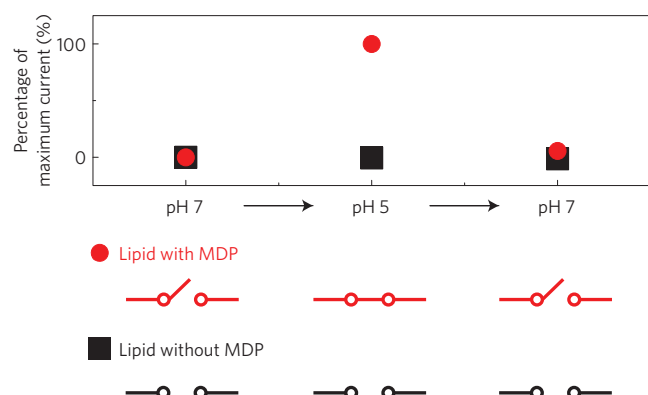


Figure 5 | Proton switch evaluation. Percentage of maximum current of O₂ reduction at -0.5 V by the Cu complex of BTT with lipid (black squares) and lipid with the MDP switch (red circles).

of MDP does not adversely affect the integrity of the lipid layer. This suggests that MDP does not phase segregate in DMPC at pH 5 and 7. Acids have been shown to phase segregate only when they are fully protonated, and MDP exists predominantly as charged species in our system^{44,45}.

pH-sensitive switch

The $\text{RH}_2\text{PO}_4/\text{RHPO}_4^-/\text{RPO}_4^{2-}$ equilibrium combined with the hindered proton transport by RHPO_4^- allows MDP to act as a pH-dependent switch for O₂ reduction inside the HBM. To evaluate the viability of MDP as a reversible switch for proton transport, we change the pH of the bulk solution *in situ* while monitoring the O₂ reduction activity of the Cu complex of BTT using chronoamperometry (Fig. 5 and Supplementary Fig. 12). The amount of O₂ reduction current by the catalyst increases substantially on changing the solution from pH 7 to pH 5. By acidifying the solution, the MDP proton carrier switch is turned on, increasing the flux of rate-limiting proton transfer to the catalyst, thus increasing the O₂ reduction current. The O₂ reduction activity of the catalyst is then shut down by turning off the MDP switch. Indeed, on readjusting the solution to pH 7, the O₂ reduction current decreases to within 5% of its original value at pH 7, demonstrating that MDP is a reversible switch for proton transport in a HBM (Fig. 5, red circles). In the absence of MDP, the lipid layer of the HBM effectively blocks proton transport to the catalyst. Therefore, the O₂ reduction current in the absence of MDP is not sensitive to changes in the pH of the bulk solution (Fig. 5, black squares).

Conclusions

We have constructed a system in which a proton transfer switch is used to turn on and off a molecular catalyst by controlling proton flux to the catalyst. By changing the pH of the bulk solution, the ability of MDP to act as a proton carrier inside a HBM can be controlled reversibly. The rate of proton transfer through the lipid layer in turn modulates the O₂ reduction activity of the embedded catalyst, which itself is an example of a synthetic Cu O₂ reduction catalyst supported on a Au electrode. The rational design of the BTT ligand, which is tailored to form a HBM on Au, exhibits catalytic activity similar to that of synthetic Cu O₂ reduction catalysts supported on carbon. This electrochemical platform allows the precise and independent control of both the thermodynamics and kinetics of proton transfer to a molecular catalyst. This approach can ultimately be used to acquire a unique mechanistic insight into PCET reactions in biological systems and energy conversion processes.

Methods

Chemicals were obtained from commercial sources and used without further purification unless otherwise specified. Aqueous solutions were prepared using Milli-Q water (>18 M Ω cm⁻¹). Potassium phosphate buffers (100 mM, pH 5 or 7) were sparged with Ar or O₂ for 30 min before each experiment.

Electrochemical studies were carried out using a CH Instruments 760 D Electrochemical Workstation (Austin, TX). For studies in aqueous and ethanolic solutions a three-electrode cell was used with a Pt wire counter electrode. Electrochemical potentials are measured and reported with respect to a no-leak Ag/AgCl/3 M KCl reference electrode. The onset potential of O₂ reduction is defined as the potential at which 5% of the maximum current is reached.

Glassy carbon electrodes were polished with alumina (0.05 μm) and sonicated in water before use. Au working electrodes were deposited using an electron-beam vacuum deposition apparatus. A Cr adhesion layer (20 nm), followed by a Au layer (250 nm), was deposited on Pyrex glass slides. The electrodes were rinsed with water and EtOH before use.

Self-assembled monolayers (SAMs) of the Cu catalysts were attached to the Au working electrodes in three steps. The thiol group was deprotected to give free BTT by adding the tritylated thiol (1.0 mg) to neat trifluoroacetic acid (100 μl), resulting in a yellow solution. Triethylsilane (~ 100 μl) was added dropwise until the solution became colourless. The resulting solution was then diluted with Ar-sparged EtOH (7.0 ml). The Au electrodes were immersed in the BTT solution for 2 h and washed with EtOH. The BTT-Au surfaces were immersed in an ethanolic $\text{Cu}(\text{ClO}_4)_2$ solution (6.7 mM) for 1 h. The electrodes were rinsed three times with EtOH and three times with pH 7 buffer solution. The Cu complex of BTT was embedded in a HBM using a previously reported procedure with pure DMPC or DMPC with one equivalent of mono-*N*-dodecyl phosphate relative to DMPC (ref. 20).

Rotating ring-disk electrode experiments were performed using a ring-disk assembly with an interchangeable disk (E5 series, Pine instruments) connected to a MSR-X rotator (Pine instruments) set to 400 r.p.m. The Au disk electrode was polished sequentially with 9 μm , 3 μm , 1 μm , 0.25 μm and 0.05 μm diameter diamond polish (Buehler) and sonicated in water after each stage. The Pt ring electrode was cleaned electrochemically by cycling from -400 mV to $+1700$ mV at 100 mV/s in an aqueous solution of HClO_4 (0.1 M) until the current of oxide stripping at ~ 350 mV remained constant. A glassy carbon electrode was used as a standard for the two-electron reduction of O₂, which has been described previously⁴⁶. The collection efficiency of the ring electrode, which was held at $+710$ mV, was determined to be 15.5%. For all reported data, the ratio of ring current to disk was obtained at -500 mV.

Chronoamperometry was performed in O₂-saturated pH 7 buffer solutions (2.6 ml). The pH of the solution was adjusted to 5 *in situ* with an Ar-sparged solution of H₃PO₄ (15 μl). The pH of the solution was adjusted back to 7 with an Ar-sparged solution of KOH (15 μl). An Ar-sparged solution of pH 7 buffer (15 μl) was added instead of acid or base in control experiments. Before and after chronoamperometry, blocking experiments with a solution of K₃Fe(CN)₆ were performed to confirm that the integrity of the lipid layer of the HBM is not compromised. A separate control experiment in which an Ar-sparged solution of pH 7 buffer (15 μl) was added twice before the addition of an Ar-sparged solution of H₃PO₄ (15 μl) further demonstrated that the increase in O₂ reduction current at pH 5 is not due to degradation of the HBM (Supplementary Fig. 12b). To evaluate the proton switch, differences in the percentage change in current before and 5 s after addition were calculated. These values were then normalized for the percentage change in current observed in the control experiments with an added Ar-sparged solution of pH 7 buffer.

Received 21 September 2013; accepted 28 March 2014;
published online 11 May 2014

References

- Browne, W. R. & Feringa, B. L. Making molecular machines work. *Nature Nanotech.* **1**, 25–35 (2006).
- Balzani, V., Credi, A., Raymo, F. M. & Stoddart, J. F. Artificial molecular machines. *Angew. Chem. Int. Ed.* **39**, 3348–3391 (2000).
- Hirjibehedin, C. F. *et al.* Large magnetic anisotropy of a single atomic spin embedded in a surface molecular network. *Science* **317**, 1199–1203 (2007).
- Fuentes, N. *et al.* Organic-based molecular switches for molecular electronics. *Nanoscale* **3**, 4003–4014 (2011).
- Alberts, B. *et al.* *Molecular Biology of the Cell* 4th edn (Garland Science, 2002).
- Von Lintig, J., Kiser, P. D., Golczak, M. & Palczewski, K. The biochemical and structural basis for trans-to-cis isomerization of retinoids in the chemistry of vision. *Trends Biochem. Sci.* **35**, 400–410 (2010).
- Donaldson, J. & Segev, N. *Trafficking Inside Cells: Pathways, Mechanisms and Regulation* (Landes Bioscience and Springer Science, 2009).

8. Lee, H. J., Gennis, R. B. & Ådelroth, P. Entrance of the proton pathway in *cbh₃*-type heme-copper oxidases. *Proc. Natl Acad. Sci. USA* **108**, 17661–17666 (2011).
9. Mayer, J. M. Proton-coupled electron transfer: A reaction chemist's view. *Annu. Rev. Phys. Chem.* **55**, 363–390 (2004).
10. Chen, Z., Vannucci, A. K., Concepcion, J. J., Jurss, J. W. & Meyer, T. J. Proton-coupled electron transfer at modified electrodes by multiple pathways. *Proc. Natl Acad. Sci. USA* **108**, E1461–E1469 (2011).
11. Huynh, M. H. V. & Meyer, T. J. Proton-coupled electron transfer. *Chem. Rev.* **107**, 5004–5064 (2007).
12. Wenger, O. S. Proton-coupled electron transfer with photoexcited metal complexes. *Acc. Chem. Res.* **46**, 1517–1526 (2013).
13. Thorseth, M. A., Tornow, C. E., Tse, E. C. M. & Gewirth, A. A. Cu complexes that catalyze the oxygen reduction reaction. *Coord. Chem. Rev.* **257**, 130–139 (2013).
14. Boulatov, R., Collman, J. P., Shiryayeva, I. M. & Sunderland, C. J. Functional analogues of the dioxygen reduction site in cytochrome oxidase: mechanistic aspects and possible effects of Cu_B. *J. Am. Chem. Soc.* **124**, 11923–11935 (2002).
15. Thorseth, M. A., Letko, C. S., Rauchfuss, T. B. & Gewirth, A. A. Dioxygen and hydrogen peroxide reduction with hemocyanin model complexes. *Inorg. Chem.* **50**, 6158–6162 (2011).
16. Oberst, J. L., Thorum, M. S. & Gewirth, A. A. Effect of pH and azide on the oxygen reduction reaction with a pyrolyzed Fe phthalocyanine catalyst. *J. Phys. Chem. C* **116**, 25257–25261 (2012).
17. Rosenthal, J. & Nocera, D. G. Role of proton-coupled electron transfer in O–O bond activation. *Acc. Chem. Res.* **40**, 543–553 (2007).
18. Chng, L. L., Chang, C. J. & Nocera, D. G. Catalytic O–O activation chemistry mediated by iron heme porphyrins with a wide range of proton-donating abilities. *Org. Lett.* **5**, 2421–2424 (2003).
19. Thorseth, M. A., Letko, C. S., Tse, E. C. M., Rauchfuss, T. B. & Gewirth, A. A. Ligand effects on the overpotential for dioxygen reduction by tris(2-pyridylmethyl)amine derivatives. *Inorg. Chem.* **52**, 628–634 (2013).
20. Hosseini, A. *et al.* Hybrid bilayer membrane: A platform to study the role of proton flux on the efficiency of oxygen reduction by a molecular electrocatalyst. *J. Am. Chem. Soc.* **133**, 11100–11102 (2011).
21. Plant, A. L. Self-assembled phospholipid/alkanethiol biomimetic bilayers on gold. *Langmuir* **9**, 2764–2767 (1993).
22. Plant, A. L. Supported hybrid bilayer membranes as rugged cell membrane mimics. *Langmuir* **15**, 5128–5135 (1999).
23. Twardowski, M. & Nuzzo, R. G. Molecular recognition at model organic interfaces: Electrochemical discrimination using self-assembled monolayers (SAMs) modified via the fusion of phospholipid vesicles. *Langmuir* **19**, 9781–9791 (2003).
24. Twardowski, M. & Nuzzo, R. G. Phase dependent electrochemical properties of polar self-assembled monolayers (SAMs) modified via the fusion of mixed phospholipid vesicles. *Langmuir* **20**, 175–180 (2004).
25. Thorum, M. S., Yadav, J. & Gewirth, A. A. Oxygen reduction activity of a copper complex of 3,5-diamino-1,2,4-triazole supported on carbon black. *Angew. Chem. Int. Ed.* **48**, 165–167 (2009).
26. Devaraj, N. K., Decreau, R. A., Ebina, W., Collman, J. P. & Chidsey, C. E. D. Rate of interfacial electron transfer through the 1,2,3-triazole linkage. *J. Phys. Chem. B* **110**, 15955–15962 (2006).
27. Inman, C. E., Reed, S. M. & Hutchison, J. E. *In situ* deprotection and assembly of *s*-tritylalkanethiols on gold yields monolayers comparable to those prepared directly from alkanethiols. *Langmuir* **20**, 9144–9150 (2004).
28. Ermakova, T. G. *et al.* Polarographic reduction of 1-substituted 1,2,4-triazoles. *Chem. Heterocyc. Compd.* **16**, 313–315 (1980).
29. Hosseini, A. *et al.* Ferrocene embedded in an electrode-supported hybrid lipid bilayer membrane: A model system for electrocatalysis in a biomimetic environment. *Langmuir* **26**, 17674–17678 (2010).
30. Rowe, G. K. & Creager, S. E. Interfacial solvation and double-layer effects on redox reactions in organized assemblies. *J. Phys. Chem.* **98**, 5500–5507 (1994).
31. Subczynski, W. K. & Hyde, J. S. Concentration of oxygen in lipid bilayers using a spin-label method. *Biophys. J.* **41**, 283–286 (1983).
32. Windrem, D. A. & Plachy, W. Z. The diffusion-solubility of oxygen in lipid bilayers. *Biochim. Biophys. Acta* **600**, 655–665 (1980).
33. Chang, P. & Wilke, C. R. Some measurements of diffusion in liquids. *J. Phys. Chem.* **59**, 592–596 (1955).
34. Jain, M. K. *Introduction to Biological Membranes* 2nd edn (Wiley, 1988).
35. Collman, J. P. *et al.* A cytochrome c oxidase model catalyzes oxygen to water reduction under rate-limiting electron flux. *Science* **315**, 1565–1568 (2007).
36. Collman, J. P. *et al.* Role of a distal pocket in the catalytic O₂ reduction by cytochrome c oxidase models immobilized on interdigitated array electrodes. *Proc. Natl Acad. Sci. USA* **106**, 7320–7323 (2009).
37. Srivastava, A., Singh, S. & Krishnamoorthy, G. Rapid transport of protons across membranes by aliphatic amines and acids. *J. Phys. Chem.* **99**, 11302–11305 (1995).
38. Schönfeld, P., Schild, L. & Kunz, W. Long-chain fatty acids act as protonophoric uncouplers of oxidative phosphorylation in rat liver mitochondria. *Biochim. Biophys. Acta* **977**, 266–272 (1989).
39. McConnell, H. M. & Kornberg, R. D. Inside–outside transitions of phospholipids in vesicle membranes. *Biochemistry* **10**, 1111–1120 (1971).
40. Palermo, E. F., Lee, D.-K., Ramamoorthy, A. & Kuroda, K. Role of cationic group structure in membrane binding and disruption by amphiphilic copolymers. *J. Phys. Chem. B* **115**, 366–375 (2010).
41. Albrecht, O., Gruler, H. & Sackmann, E. Polymorphism of phospholipid monolayers. *J. Phys. France* **39**, 301–313 (1978).
42. John, K., Schreiber, S., Kubelt, J., Herrmann, A. & Müller, P. Transbilayer movement of phospholipids at the main phase transition of lipid membranes: Implications for rapid flip–flop in biological membranes. *Biophys. J.* **83**, 3315–3323 (2002).
43. Han, X., Wang, L., Qi, B., Yang, X. & Wang, E. A strategy for constructing a hybrid bilayer membrane based on a carbon substrate. *Anal. Chem.* **75**, 6566–6570 (2003).
44. Mercado, F. V., Maggio, R. & Wilke, N. Phase diagram of mixed monolayers of stearic acid and dimyristoylphosphatidylcholine. Effect of the acid ionization. *Chem. Phys. Lipids* **164**, 386–392 (2011).
45. Mercado, F. V., Maggio, R. & Wilke, N. Modulation of the domain topography of biphasic monolayers of stearic acid and dimyristoyl phosphatidylcholine. *Chem. Phys. Lipids* **165**, 232–237 (2012).
46. Gong, K., Du, F., Xia, Z., Durstock, M. & Dai, L. Nitrogen-doped carbon nanotube arrays with high electrocatalytic activity for oxygen reduction. *Science* **323**, 760–764 (2009).

Acknowledgements

C.J.B. acknowledges a National Science Foundation Graduate Research Fellowship (NSF DGE-1144245) and a Springborn Fellowship. E.C.M.T. acknowledges a Croucher Foundation Scholarship. We thank Michael Cason for his assistance in preparing Au on glass substrates. We thank the US Department of Energy (DE-FG02-95ER46260) for support of this research. This work was carried out in part in the Frederick Seitz Materials Research Laboratory Central Facilities, which are partially supported by the US Department of Energy (DE-FG02-07ER46453 and DE-FG02-07ER46471).

Author contributions

C.J.B., E.C.M.T., S.C.Z., A.H. and A.A.G. designed the experiments. C.J.B., E.C.M.T. and T.B.S. performed the experiments. Y.L. synthesized BTT. C.J.B., E.C.M.T., Y.L., S.C.Z., A.H. and A.A.G. wrote the paper. C.J.B., E.C.M.T., A.H. and A.A.G. analysed the data. All authors discussed the results and commented on the manuscript.

Additional information

Supplementary information is available in the online version of the paper. Reprints and permissions information is available online at www.nature.com/reprints. Correspondence and requests for materials should be addressed to A.A.G.

Competing financial interests

The authors declare no competing financial interests.